Applied Physics B (2018) 124:68
https://doi.org/10.1007/s00340-018-6939-4

Applied Physics B
Lasers and Optics

Terahertz multiband ultrahigh index metamaterials by bilayer metallic grating structure

Xincui Gui[1] · Xufeng Jing[1] · Pengwei Zhou[1] · Jianjun Liu[2] · Zhi Hong[2]

Received: 7 August 2017 / Accepted: 29 March 2018 / Published online: 3 April 2018

Abstract
One-dimensional metallic grating structure was proposed to realize high refractive index metamaterial in the terahertz region. By drastically increasing the effective permittivity by means of intense capacitive coupling and reducing the diamagnetic effect using a thin metallic thickness, a peak refractive index of 15.81 at the resonant frequency in embedded metallic grating can be obtained. Multiband high refractive index metamaterial can be realized by double symmetric metallic grating and asymmetric grating structure. For asymmetric grating metamaterial structure, two separate transmission peaks appear and result in two separate high refractive index. Interestingly, a near zero refractive index metamaterial can be obtained by the introduction of double asymmetric design. It was found that our designed ultrahigh refractive index metamaterials depend on the electric field coupling effect and the magnetic field diamagnetic response.

1 Introduction

Recently, metal-dielectric structures have attracted a huge amount of attention due to its extraordinary electromagnetic properties such as subwavelength resolution or the possibility to construct an invisibility device [1].In these fields, it is very intriguing and extremely useful for creating an artificial medium with free controlled refractive index ($n = \sqrt{\varepsilon\mu}$) [2]. Also, it is great importance for imaging, lithography, compact optical circuits, and miniaturized electromagnetic devices [3].For example, the resolution of microscope system is inversely proportional to refractive index ($\mathrm{NA} = n * \sin\alpha$) [4, 5]. Increasing refractive index of material over a large frequency range results in broadband slow light effect, which can be used to enhance the storage capacity of the delay lines [6].High index metamaterials can also enhance the spectral sensitivity of certain types of interferometers and can benefit many other practical application areas [6]. And Terahertz continuous wave sources, such as resonant tunneling diodes (RTD) and quantum cascade lasers (QCL), will need devices with high refractive indices which can be applied in radiation structures with high directivity [7].

Previous work focused on high-impedance surfaces used as an antenna substrate [1–3], negative refractive index metamaterials [8, 9], effective surface plasmon behavior [10, 11] on perfect metallic surface with gratings [12], and effective bulk plasmon behavior in thin-wire structures [9]. On the contrary, it was found that the opposite side-high refractive index metamaterial attracts far less attention. Recently, Shin et al. demonstrated numerically the mechanisms of a broadband high refractive index metamaterial with three-dimension (3D) structure [13], and Choi et al. proposed a two-dimensional (2D) terahertz metamaterial with unnaturally high refractive index [2] but the presented 3D and 2D structure are not easy for implementation in experiment. Therefore, we proposed a one dimensional (1D) metallic grating terahertz metamaterial to realize ultrahigh effective refractive index [14–16] and near-zero refractive index. More recently, numerous reports have appeared for metamaterials with a near-zero refractive index (NZI)in terahertz region [17, 18]. The materials which have permeability in the neighborhood of $\mu = 0$ are known as μ-near zero (MNZ) material, and the material with permittivity in the neighborhood of $\varepsilon = 0$ are referred as ε-near zero (ENZ) material. Both MNZ and ENZ have special properties. Electromagnetic waves in a material with a refractive index of zero have an infinite phase velocity and wavelength. These properties pave the way for a number of applications such as cloaking

✉ Xufeng Jing
jingxufeng@cjlu.edu.cn

[1] Institute of Optoelectronic Technology, China Jiliang University, Hangzhou 310018, China

[2] Centre for THz Research, China Jiliang University, Hangzhou 310018, China

[18], superreflection, tunnelling, funnelling, super-coupling channels and the arbitrary reshaping of phase fronts [19–21]. A performance (effective refractive index values) comparison of the proposed structure with that of the current state of the art is presented in Table 1.

In this paper, we designed high refractive index metamaterials based on metallic gratings structures in the terahertz region. By strong capacitive coupling resulting from a smaller gap width between the unit cells, the effective permittivity can be drastically increased. Through decreasing the area enclosed by the induced surface currents, the diamagnetic response of metamaterials can be reduced, resulting in the increase of effective permeability. The zero refractive index metamaterials and high index metamaterial can be realized by double asymmetric metallic grating.

Table 1 Performance comparison. The effective refractive index value of the current state of the art is compared with that of the proposed structure

Reference article	Frequency (THz)	Highest value of ref. index
Ref. [2]	0.516	27.25
Ref. [7]	0.319	8.72
Ref. [22]	0.384	61.83
Our work	1.41	15.81

2 Metamaterial design and analysis

2.1 Metallic gratings for high refractive index metamaterials

The embedded metallic grating of the proposed high refractive index metamaterial is shown in Fig. 1a, the electric field vector of an incident terahertz wave is along x direction (TM polarization). Here, the metal used to construct the metamaterials is lossy copper ($\sigma = 5.96 \times 10^7$ S/m), and the substrate is made from a dielectric polyimide material with the refractive index of $n = 1.8 + 0.04i$. The frequency

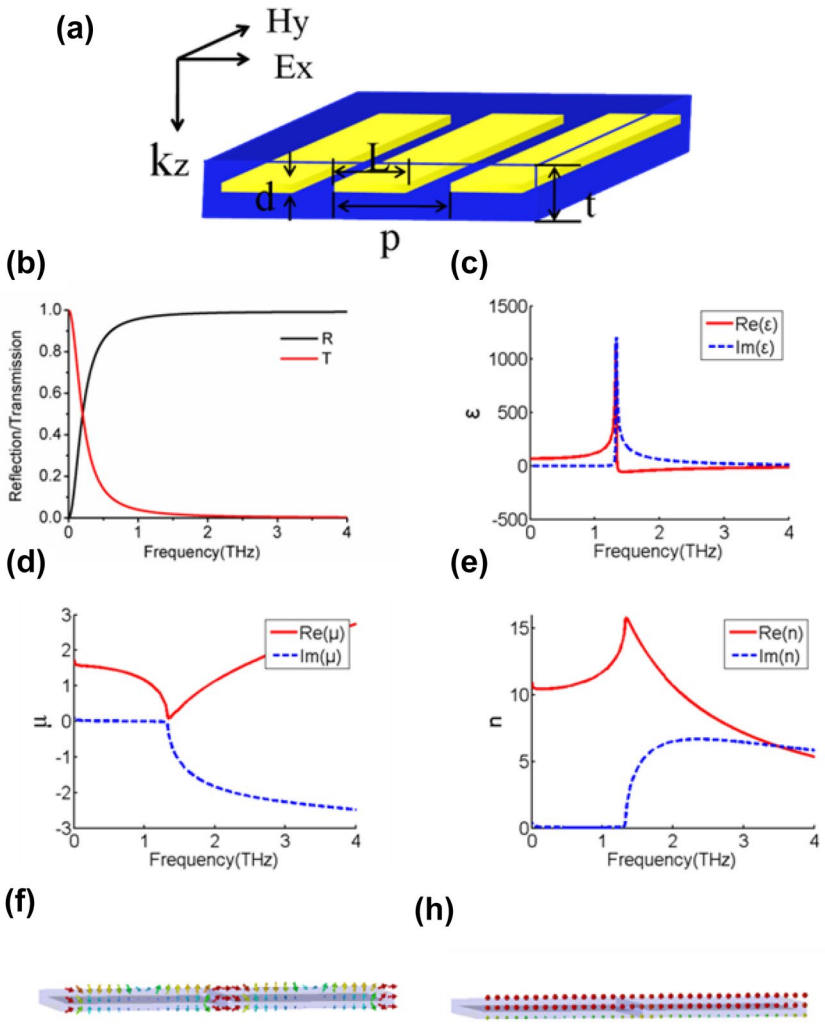

Fig. 1 **a** Schematic of unit cell structure of the high-index grating metamaterial. **b** Simulated transmission (*T*) and reflection (*R*) spectra of the structure for TM polarization, **c** extracted effective permittivity, **d** permeability, **e** refractive index for the high index metamaterial by the S-parameter retrieval method. **f** Saturated electric field distribution at 0.8 THz for the metallic grating metamaterial, the red region shows strong electric field. **h** the vector plot of the magnetic field distribution at 0.8 THz in the unit cells

dispersion of the refractive index of polyimide was ignored in this simulation. The thin metallic grating is embedded in substrate. Three-dimensional full-wave electromagnetic field simulation by finite integral method was used to accurately calculate transmission and near-field distribution.

The used geometrical parameters of the structure are $p = 60$ μm, $t = 5$ μm. The metallic structure is embedded in the substrate, and the original geometrical parameters of the metallic grating are $L = 59$ μm, $d = 0.2$ μm. To reduce the diamagnetic effect caused by the magnetic dipole that results from the current loop surrounding the structure, the designed thickness of the metallic grating is 0.2 μm. The gap width is defined by $g = p - L$. When a Terahertz wave impinge the structure, a larger amount of surface charges accumulated on the edge of the metallic patch leads to an extremely large dipole in the unit cell [22–25]. According to the amount of accumulated charge, the effective permittivity indicates different asymptotic actions that depend on the gap width [2]. When the gap width is satisfied as $g/p << 1$, a strong capacitive coupling will occur, the effective permittivity can be greatly increased.

The simulated transmission/reflection spectra for TM polarization is plotted in Fig. 1b. We extracted the constitutive parameters of grating metamaterial using a common method of *S* parameters proposed by Smith et al. [26].This method has been proved to be precise by a comparison between the theoretical estimation and the experimental extraction [27]. A strong electrical resonance is observed with a peak relative permittivity of about 1200 at the frequency near 1.41 THz, and the peak of the refractive index is 15.81. In Fig. 1d, the magnetic permeability remains a lower value near the resonant frequency, resulting in the weak magnetic anti-resonance.

To illustrate the physical properties of this high refractive index metamaterial, the electric and magnetic field around the embedded metallic grating in the two unit cells were numerically simulated at the frequency of 0.8 THz (Fig. 1f, h). In Fig. 1f, the electric field is strongly concentrated in the gap, a large amount of surface charge can be accumulated on the edge of parallel-plate capacitor because the charges in each edge of unit cell interact with opposite charges in close proximity across the gap [28]. Figure 1h shows the magnetic field penetrated deeply into the unit cell at frequencies due to the negligible metallic volume fraction subtended by current loops, leading to decrease of diamagnetic effect of metamaterial.

The gap width and the metallic thickness are the key geometrical parameters for increasing the refractive index of the metamaterial. The effect of different gap widths and the metallic thickness on refractive index are shown in Fig. 2. In Fig. 2a, it is found that the increase of gap width leads to the decrease of the effective refractive index peak, and the peak of the index makes a red-shift, resulting in a narrow

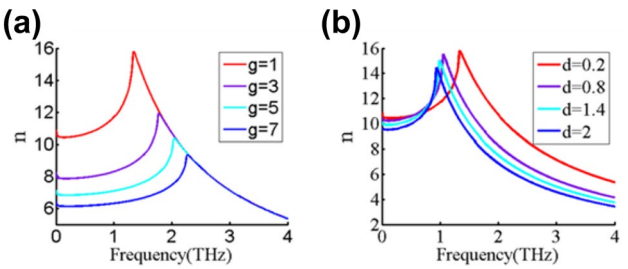

Fig. 2 Dependent transmission and effective refractive index of geometrical parameters *g* and *d*: **a** the real part of the index as a function of gap width *g*; **b** the real part of the refractive index as a function of metallic thickness *d*

bandwidth of the high refractive index at the quasi-static limit. This is because there is a great increase of the capacitance due to coupling between unit cells when the gap width decreases. In Fig. 2b, increasing the metallic thickness result in the decrease of the effective refractive index peak, and the resonance frequency shifts to lower frequency region.

2.2 Double metallic gratings for zero refractive index

For above design and analysis of the embedded metallic grating metamaterial, it is known that the experimental preparation is complex [29, 30].To obtain a simple structure with easily preparation, we designed a single-sided metallic grating metamaterial in Fig. 5. Here, the parameters of the unit cell are the same as that of the embedded metallic grating. To indicate the effect of extremely large dipole moments and weak diamagnetism in the unit cell, the effective permittivity, the effective permeability and the effective refractive index were extracted. It is found that the peak of refractive index is lower compared with the embedded grating structure. The waveform is similar to the embedded grating structure.

Figure 3 schematically illustrates a double metallic grating, resulting in multiple band high refractive index. The simulated transmission/reflection spectra for symmetric double gratings as shown in Fig. 3a, ① at TM polarization incidence is plotted in Fig. 3b. In Fig. 3a), we selected a thickness of $d = 0.2$ μm and a width $L = 59$ μm for the metallic grating ①, the substrate thickness of $t = 5$ μm, $p = 60$ μm. Two resonances in reflection and corresponding minima in transmission between 0 and 4 THz are observed. The transmission peaks are at frequencies of 1.17 and 3.5 THz. There are three peaks in the real part of refractive index in Fig. 3b, $n = 15.37$ at 1.17 THz, $n = 10.93$ at 1.65 THz and $n = 9.837$ at 3.66 THz. It proves that our structure can provide a three band high refractive index. To reveal the physical origin of the high refractive index of the metamaterial for the symmetry double metallic grating

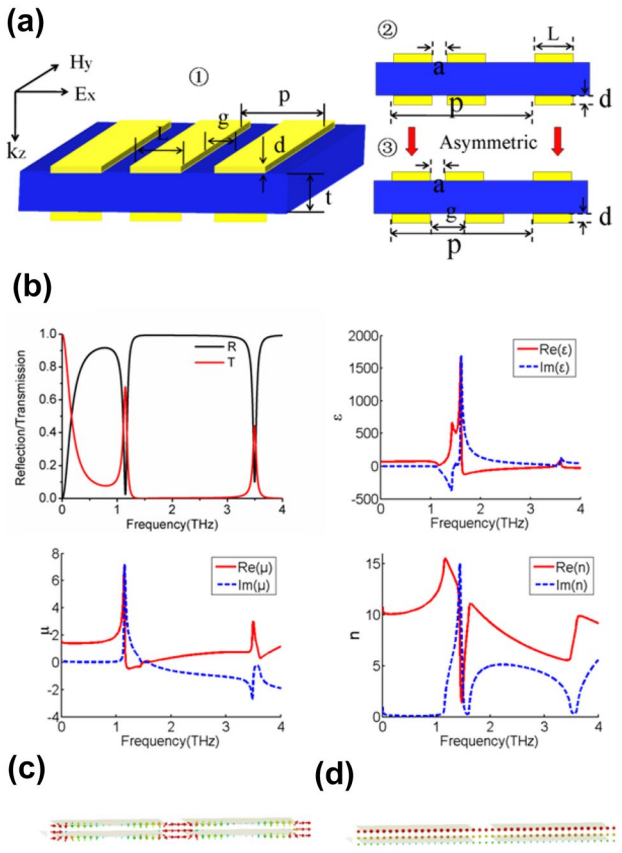

Fig. 3 **a** The structure with two metallic gratings deposited on each side of a dielectric layer ①. Three-dimensional diagram of the designed structure with two sets of metallic gratings deposited separately on both sides of dielectric layer. ②, ③ Cross-section of two different asymmetric structures and their structure parameters. **b** Simulated transmission (T) and reflection (R) spectra of the structure for TM polarization (top left), extracted effective permittivity(ε, top right) and permeability(μ, bottom left), refractive index for the high index metamaterial by the S-parameter retrieval method is shown at bottom right. **c** Electric field distribution at 0.5 THz for the symmetry double metallic grating metamaterial with two unit cells. **d** The vector plot of the magnetic field distribution at 0.5 THz in two unit cells

metamaterial. We can find that the high value of the real part of the effective refractive index (second peak) appears high permittivity, then the first and third peak of the effective refractive index appears because of high permeability and permittivity simultaneously in Fig. 3b. The electric and magnetic field around the metallic grating in the two unit cells were numerically simulated at the frequency of 0.5 THz (Fig. 3c, d). The electric field was strongly concentrated in the gap along the long side between each the symmetry double metallic grating structure on the double at 0.5 THz. This strong electric field arises extreme polarization density to provide huge effective permittivity. Obviously, because of the negligible metallic volume fraction, the magnetic field penetrates deeply into the unit cell in 0.5 THz as shown in Fig. 3d.

Then the transmission was calculated for the symmetric structure and asymmetric structures as shown in inset of Fig. 4a. Two different asymmetric structures with $a = 2$ μm appear two separate transmission peaks near 1.41 and 1.49 THz, respectively. This separate transmission peaks result in two separate high refractive index, leading to a three-band high refractive index metamaterial component. For example, for the asymmetric structure ② the refractive index are $n = 10.91$ at 1.41 THz, $n = 11.77$ at 1.47 THz, and $n = 5.86$ at 3.03 THz. Interestingly, for the asymmetric structure ② in Fig. 3a, the permeability is close to zero($-0.39 < \mathrm{Re}\ (\mu) < 0$) from 1.67 to 1.71 THz, near zero refractive index from 1.67 to 1.71 THz can be obtained, as marked in the zoomed plot of Fig. 4d. It is found that zero refractive index at 1.71 THz, and magnetic permeability is to be near zero in Fig. 4d, the permeability can be controlled through the inductance of the metallic slab width. Also, the wideband near zero refractive index property with 40 GHz bandwidth between 1.67 and 1.71 THz is revealed. As the asymmetric metallic influence increases in the structure, the effect of capacitive coupling between the adjacent unit cells structures decreases while the adjacent unit cells form a capacitor with different gap, resulting in the value of permittivity decrease. A reduced total reflectivity will result in a higher peak value of ε, leading to a more broadband behavior [31]. Such these μ-near zero (MNZ) metamaterials ($\varepsilon' > 0,\ \mu' \to 0$) are known as perfect electrical conductors. This zero refractive index metamaterials can be applied in the field of cloaking, directional antenna design [32], wave directivity [33–35] and radiation pattern [36]. Thus, these asymmetric double grating structure can realize multiband high refractive index metamaterial and near zero refractive index metamaterial.

3 Conclusion

Using one-dimensional metallic gratings structure, high refractive index can be obtained with small gap width and thin metallic thickness. For asymmetric bilayer grating structures, the multiband unnaturally high refractive index at terahertz region can be realized, and they also show wideband zero refractive index property in the terahertz region. Our findings concerning multiband high-index metamaterials and zero refractive index metamaterials can be expected to use in many functional photonic devices, such as transformation optic components.

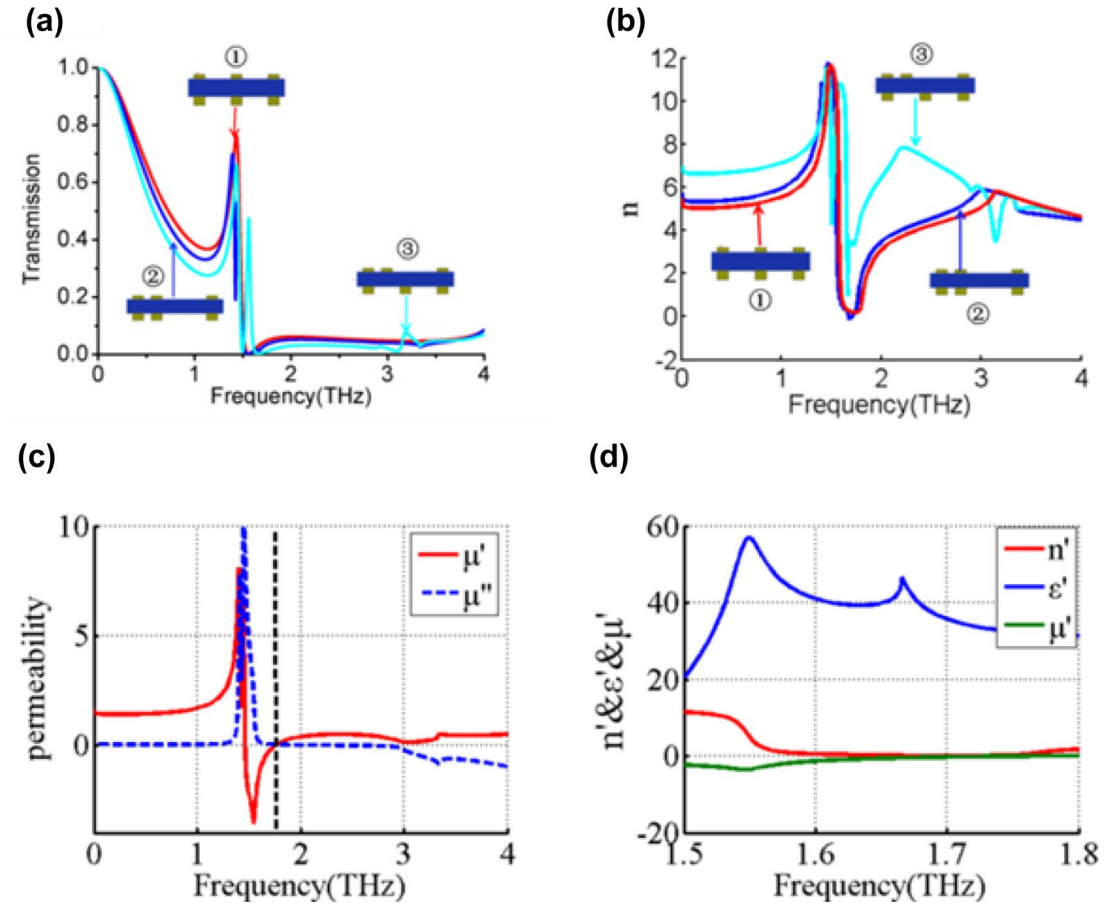

Fig. 4 **a** The typical transmission spectra of three different asymmetric structures. **b** The extracted refractive index. **c** The extracted permeability for the asymmetric structure ② in Fig. 3a. **d** Extracted the real part refractive, permittivity and permeability and for the asymmetric structure

Acknowledgements The authors acknowledge the support from Natural Science Foundation of Zhejiang Province (LY17F050009, LQ15F050004), National Natural Science Foundation of China (NSFC) (No.61505192).

References

1. Y. Liang, W. Peng, M. Lu, Chu, S, Narrow-band wavelength tunable filter based on asymmetric bilayer metallic grating. Opt. Express **23**(11), 14434 (2015)
2. M. Choi., S.H. Lee, Y. Kim, S.B. Kang, J. Shin., M.H Kwak, A terahertz metamaterial with unnaturally high refractive index". Nature **470**(7334), 369 (2011)
3. X. Wei., H. Shi., X. Dong., Y. Lu., C. Du, A high refractive index metamaterial at visible frequencies formed by stacked cut-wire plasmonic structures. Appl. Phys. Lett. **97**(1), 011904-011904-3 (2010)
4. D.V.P. Xiao. Shumin, A.V. Kildishev, X. Ni., U.K. Chettiar, H.K. Yuan, Loss-free and active optical negative-index metamaterials. Nature, 466(7307):735 (2010)
5. R. Singh, W. Singh, W. Zhang, Ultra-high terahertz index in deep subwavelength coupled bi-layer free-standing flexible metamaterials. J. Appl. Phys. 121.23:2075–329 (2017)
6. Z. Shi, R.W. Boyd, R.M. Camacho, P.K. Vudyasetu, J.C. Howell, Slow-light fourier transform interferometer. Phys. Rev. Lett., 99(24):240801 (2007)
7. K. Ishihara, T. Suzuki, Metamaterial demonstrates both a high refractive index and extremely low reflection in the 0.3-THz Band. J. Infrared Millimeter Terahertz Waves, 1–10 (2017)
8. R. Liu., C. Ji., J.J. Mock., J. Chin, T.J. Cui, D.R. Smith, Broadband ground-plane cloak. Science **323**(5912), 366–369 (2009)
9. M. Zhong, Influence of dielectric layer on negative refractive index and transmission of metal-dielectric-metal sandwiched metamaterials. Chin. Optics Lett. **12**(4), 51–53 (2014)
10. F.J. Garciavidal, L. Martinmoreno, J.B. Pendry, Surfaces with holes in them: new plasmonic metamaterials. J. Optics A Pure Appl. Optics **7**(2), S97 (2005)
11. A.P. Hibbins, B.R. Evans, J.R. Sambles, Experimental verification of designer surface plasmons. Science **308**(5722), 670 (2005)
12. J.B. Pendry., D. Schurig, D.R. Smith, J.B. Pendry, D. Schurig, Smith, D. R, Controlling electromagnetic fields. Science **312**, 1780–1782, Science, 312(5781), p. 1780–1782. (2006)

13. J. Shin, J.T. Shen, S. Fan, Three-dimensional meta-materials with an ultra-high effective refractive index over broad bandwidth. Phys. Rev. Lett. **102**(9), 093903 (2009)
14. D. Sun, M. Wang, Y. Huang, Y. Zhou, M. Qi, M. Jiang, Z. Ren, Enhanced spatial terahertz modulation based on graphene metamaterial". Chin. Optics Lett. **15**(5), 051603 (2017)
15. W. Wang, F. Yan, S. Tan, H. Zhou, Y. Hou, Ultrasensitive terahertz metamaterial sensor based on vertical split ring resonators". Photonics Res. **5**(6), 571–577 (2017)
16. W. Zhu, M. Jiang, H. Guan, J. Yu, H. Lu, J. Zhang, Z. Chen, Tunable spin splitting of Laguerre–Gaussian beams in graphene metamaterials. Photonics Res. **5**(6), 684–688 (2017)
17. S.C.A. Sonsilphong, N. Wongkasem, "Meta-materials with near-zero refractive index produced using fishnet structures. J. Opt. **16.1**, 100–103 (2013)
18. S.D. Mock. J.J. Justice, S.A Cummer, J.B. Pendry, A.F. Starr, Metamaterial electromagnetic cloak at microwave frequencies. Science **314**(5801), 977–80 (2006)
19. K. Konstantinidis, A.P. Feresidis, Broadband near-zero index metamaterials. J. Optic, 17.10:105104 (2015)
20. M. Dubois., C. Shi., X. Zhu., Y. Wang., X. Zhang, Observation of acoustic dirac-like cone and double zero refractive index. Nat. Commun., **8**:14871 (2017)
21. R. Vukoman, ČolovićB. Jokanović, Miloš Nenadovič, Anka Trajkovska Petkovska, Mitrić. M, & B. Jokanović, Ultra-high and near-zero refractive indices of magnetron sputtered thin-film metamaterials based on TixOy. Adv. Mater. Sci. Eng., 7–8 (2016)
22. Z. Lu, B. Campsraga, N.E. Islam, Design and Analysis of a THz metamaterial structure with high refractive index at two frequencies. Physics Research International, pp. 2090–2220 (2012)
23. G. Litmanovitch, D. Rrotshild, A. Abramovich, Flat mirror for millimeter-wave and terahertz imaging systems using an inexpensive metasurface. Chin Optics Lett **15**(1), 011101 (2017)
24. L. Bibbò, K. Khan, Q. Liu, M. Lin, Q. Wang, Z. Ouyang, Tunable narrowband antireflection optical filter with a metasurface. Photonics Res **5**(5), 500–506 (2017)
25. Z. Bai, G. Tao, Y. Li, J. He, K. Wang, G. Wang, X. Jiang, J. Wang, W. Blau, L. Zhang, Fabrication and near-infrared optical responses of 2D periodical Au/ITO nanocomposite arrays. Photonics Res **5**(4), 280–286 (2017)
26. D.R. Smith, S. Schultz, P. Marko, C.M. Soukoulis, Determination of effective permittivity and permeability of metamaterials from reflection and transmission coefficients. Phys. Rev B., 65(19), 195104 (2001)
27. X. Jing, W. Wang, R. Xia, J. Zhao, Y. Tian, Z. Hong, Manipulation of dual band ultrahigh index metamaterials in the terahertz region". Appl. Opt., **55**(31), 8743 (2016)
28. X. Jing, X.C. Gui, R. Xia., Z. Hong, Ultrabroadband unnaturally high effective refractive index metamaterials in the terahertz regio. IEEE Photonics J. **PP**(99), 1–1 (2017)
29. A. Darweesh. Ahmad, S.J. Bauman, J.B. Herzog, Improved optical enhancement using double-width plasmonic gratings with nanogaps. Photonics Res., 4.5:173 (2016)
30. X.R. Shi., Y. Guo., R. Chen., T. Hao. L, & Chen, X, Periodic structural defects in Bragg gratings and their application in multiwavelength devices. Photonics Res., 4.2:35 (2016)
31. K. Konstantinidis, A.P. Feresidis, Broadband near-zero index metamaterials. J. Opt. **17**(10), 105104 (2015)
32. S. Islam., M. Faruque, M. Islam, A near zero refractive index metamaterial for electromagnetic invisibility cloaking operation. Materials **8**(8), 4790–4804 (2015)
33. H. Zhou, P. Zhibin, S. Qu, S. Zhang, J. Wang, Z. Duan, H. Ma, Z. Xu, A novel high-directivity microstrip patch antenna based on zero index metamaterial. IEEE Antennas Propag. Lett. 8, 538–541 (2009)
34. M. Silveirinha, N. Engheta, Tunneling of electromagnetic energy through subwavelength channels and bends using ε-near-zero materials. Phys. Rev. Lett. **97**, 157 403 (2006)
35. R. Lui, Q. Cheng, T. Hand, J.J. Mock, T.J. Cui, S.A. Cummer, D.R. Smith, Experimental demonstration of electromagnetic tunneling through an epsilon-near-zero metamaterial at microwave frequencies. Phys. Rev. Lett. **100**, 023903 (2008)
36. B. Wang, K.-M. Huang, Shaping the radiation pattern with mu and epsilon—near-zero metamaterials. Progress Electromagn. Research **106**, 107–119 (2010)